Solid Freeform Fabrication 2021: Proceedings of the 32nd Annual International Solid Freeform Fabrication Symposium – An Additive Manufacturing Conference
Reviewed Paper

STUDY OF SPATTER FORMATION AND EFFECT OF ANTI-SPATTER LIQUID IN LASER POWDER BED FUSION PROCESSED Ti-6Al-4V SAMPLES

A. Ganesh-Ram*, M. Hanumantha*, B. B. Ravichander*, B. Farhang*, S. Ramachandra*, N. Shayesteh Moghaddam*, A. Amerinatanzi*†

*Mechanical & Aerospace Engineering, University of Texas at Arlington, Arlington, TX.
†Materials Science and Engineering, University of Texas at Arlington, Arlington, TX.

Abstract

Spatter deposition has been found to have serious effects on mechanical properties of the metal parts printed using laser powder bed fusion technique. The spatter powder formation can cause unfavorable changes in phases and impurity content and may result in the formation of defects in the as-fabricated parts. This study is the first of its kind focusing on mitigation of spatter formation through a novel technique of spraying nonflammable welding liquid during the LPBF process. Identifying the spatter particle size distribution and dampening its formation have been the focus of this study. Characterization of the powder spatter behaviors for Ti-6Al-4V have been made through image processing and microstructure characterization. The findings of this study will help in improving the mechanical properties and reducing the post-processing procedures required for the parts processed by LPBF. This study is believed to bring a new perspective in production planning and print quality optimization to obtain an enhanced performance from laser powder bed fusion technique.

Keywords: Laser powder bed fusion, Ti-6Al-4V, Spattering, Anti-Spatter Liquid.

1. Introduction

Ti-6Al-4V alloy is one of the earliest alloy developed with Titanium [1]. It has a lower density, but relatively high strength compared to other alloys. Initially developed for aircraft structures, its field of applications diversified [2]. Biocompatibility and corrosion resistant property of the alloy makes it commonly used for orthopedic and dental implants [3]. The α+β combination phase of this alloy contributes towards its strength and the amount of α and β phases depend on the heat treatment cycles that are carried out [4]. High demand for the alloy makes it expensive and hence conventional manufacturing which involves machining adds up to its cost with material wastage. With the capability of using Laser Powder Bed Fusion (LPBF) process to fabricate the parts with Ti-6Al-4V alloy, a new dimension of applications could be realized. Further the formation of mesostructures during LPBF of the alloy gives an advantage for development of harder parts [5]. Ductility and toughness property have also been found to be preserved for the LPBF processed alloy [6].

In a LPBF process, when the metal powder gets melted upon focusing the laser beam, it becomes molten metal. The molten metal is uncontrollable because of the energy being concentrated over that small volume of the powder. Heating and cooling rate affects the quality of the solid that gets developed out of it. The mechanical property of the printed part depends on the fusion of molecules that takes place in the melt pool when it cools down [7]. Spatter formation is one of the drawbacks that affects the mechanical properties of the fabricated part, as the particles get trapped within the built part and voids that it create degrades the strength of the part [8]. The evaporation of the metal from the molten pool gives rise to a pressure termed as recoil pressure which then determines the shape of the melt pool [9] The recoil pressure is directly proportional to the amount of metal evaporated, while a lower pressure flattens the surface of the melt pool higher pressure corroborates expulsion of molten metal as spatters. The spatters are formed due to uncontrolled recoil pressure, surface tension and Marangoni effect over the surface of the molten melt pool [8].

Fewer studies have been carried out to analyze the spatter formation in the LPBF process. Andani *et al.* [10] observed the behavior of spatter during a LPBF process using a high speed camera for a double laser processing of the metal powder and concluded that increasing the number of lasers has a direct effect in raising the amount of spatters formed . It has been found that the amount of spatter is dependent on the laser power as well as the powder material [11]. In another study by the same group, it was confirmed that increasing the laser width and reducing the volume energy density suppressed the spatter formation. Nasab *et al*. [12] compared the microstructure of the spatter with that of the LPBF processed part and concluded that the microstructure was coarse when compared with the former. These studies suggested that the spatter powder can be mitigated to some extent by appropriate changes in laser process parameters. However, the other in-situ mitigating approach has not been investigated.

In this study, the effect of spraying an anti-spattering liquid (ASL) to the as-received powder prior to LPBF was also investigated. Based on the results obtained, spraying the ASL has a minimum effect on the as-received powders after the fabrication while they significantly decrease the size and number of spatter powder during the fabrication.

2. Materials and Methods

2.1 Powder and Anti Spatter Liquid

The as-received metal powder in this study was Ti-6Al-4V, which was obtained from EOS GmbH. To avoid inhomogeneity and secure uniform particle size distribution, the powder was sieved prior to the LPBF fabrication. Average powder particle size ranging from 35 µm to 45 µm was determined using SEM analysis for the as-received powder. The composition and weight percentages of main elements in the powder are reported in Table 1.

Table 1. Composition of elements in the Ti-6Al-4V powder material purchased from EOS.

Element	Ti	Al	V	O	N	C	H	Fe
Concentration	Balance	5.5 – 6.75 wt.%	3.5 – 4.5 wt.%	< 2000 ppm	< 500 ppm	< 800 ppm	< 150 ppm	< 3000 ppm

To study the influence of adding anti-spatter liquid (ASL) to the as-received Ti-6Al-4V powder, aimed at mitigating the powder spatter formation, Walter E-weld 4^{TM} (Walter Surface Technologies, Windsor, CT) anti-spatter liquid was used. This affected powder will be referred to as ASLed powder throughout this manuscript. The chemical and physical properties of the ASL are reported in table 2.

Table 2. Chemical and physical properties of E-weld 4^{TM} Anti spatter liquid.

Chemical composition	Polyethylene Glycol
Flammability	Not Flammable
pH	9
Melting point	0°C (32°F)
Boiling point	98°C (208.4°F)
Density	0.99 g/ml @ 20°C (68°F)

2.2 Fabrication

Two LPBF runs were programmed and carried out to investigate the influence of adding ASL to the as-received powder. One run was conducted using the as-received Ti-6Al-4V powder, and the other run was done after spraying a controlled amount of ASL to the as-received powder. The LPBF process was carried out in an EOS M290 DMLS metal 3D printer equipped with a 400 W Ytterbium fiber laser. The employed process parameters were laser power (P) of 250 Watt, scanning speed (v) of 1.25 m/s, hatch spacing (h) of 120 μm and a layer thickness of 40 μm. Test parts with 3 mm length, 5 mm in height and 2 mm in width were created for this study.

2.3 Anti-Spatter Liquid and Spray System

A spray system, capable of pumping the ASL liquid from its reservoir and spraying it through its fogger, was manually built and placed inside the EOS M290 build chamber. The system's components were connected using ½ inch polymer tubes. In order to pump the ASL liquid from the reservoir to the fogger, a 12 V DC mini pump operable with batteries were used. The spray system was set up in such a way that the fogger can fine spray a specific quantity of the liquid over each deposited as-received powder layer whenever the pump is manually initiated.

2.4 High Speed Image Capturing and Processing

A high-speed Fastcam Mini UX100 camera was used to capture the spatter formation at 2000 frames per second while the laser processes either the as-received or ASLed powder during

both the runs. The camera was setup such that it's focus was on the region of interest, i.e., the region where the laser interacts with the powder, as shown in figure 1. Image processing was then performed in the ImageJ package developed by the National Institute of Health and was used to find the number of spatters formed while the laser processed the as-received and ASLed powder [13].

Figure 1. The camera setup outside the EOS M290 process chamber.

A image thresholding technique developed by Otsu was used to identify only the required gray regions [14] for laser spot and spatter particles. It is interesting to note that when the laser passes a scan path and moves on to the next path, spatters that would have been formed from the previous path would still be in the image before it falls back to the powder layer. Therefore, the images obtained by the camera were then cleaned by manually identifying the spatter particles that were formed from previously scanned paths and ignoring them. Then the image frames were obtained at 2 ms intervals from processing the as-received powder and ASLed powder were matched such that images were taken during a specific scanning paths of the laser at both the cases. After that the number and size of the spatters found in images captured during either run were recorded. The spatter particles of area less than 5 μm^2 were not considered in the count.

2.5 Microstructure and Compositional Analysis

SEM Micrographs of the as-received and ASLed powder were obtained using Hitachi S-3000N variable pressure SEM. The XRD results of both the as-received and ASLed powders were also obtained using Bruker D8 advance X-ray Diffractometer.

3. Results and Discussion

3.1 Spatter Particle Capture and Image Processing

The images captured by the high-speed camera during the LPBF processing of both the as-received and ASLed powders are presented in figures 2 and 3, respectively. Images from both runs have been obtained and picked such that the scan paths at which the images were captured were the same. In every image, the spatter particles that were seen from the previous image for the same laser scan path was made sure to be eliminated before counting the spatter particles. As can be

seen from the figures 2 and 3, spatter powders were ejected from the spot where laser melts the powder. It was also noted that there was a variation in size of the spatters.

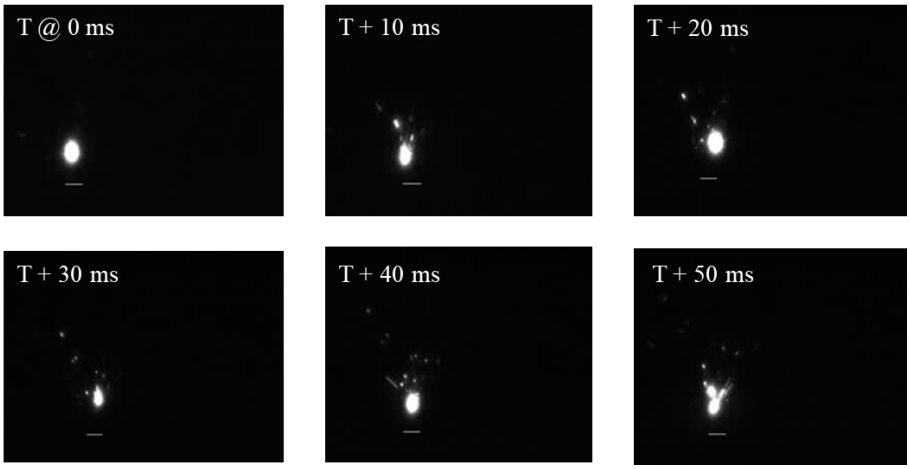

Figure 2. Images captured during LPBF run over as-received powder at 10 ms intervals.

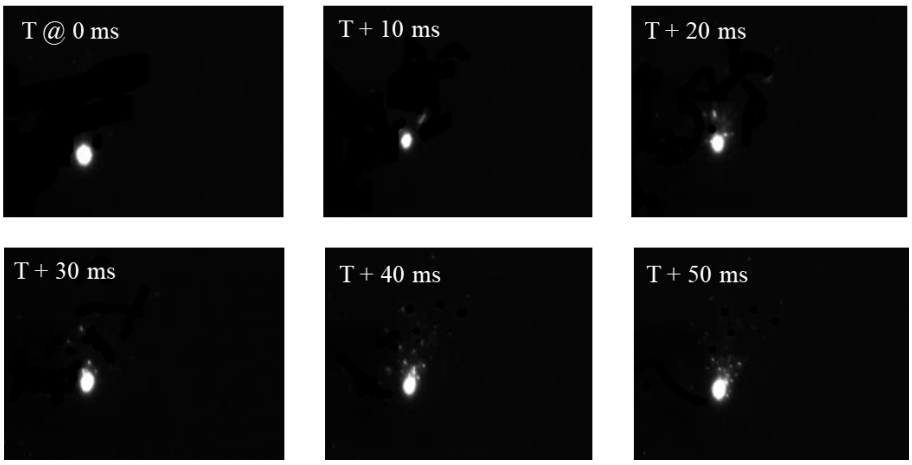

Figure 3. Images captured during LPBF run over ASLed powder at 10 ms intervals.

A detailed comparison of images from both the runs was made in figure 4. The spatters that were ejected as well as the laser spot were indicated in the images for a better identification. A clear reduction in number of spatter particles ejected out of the melt pool have been observed when comparing figure 4 b) with figure 4 a). A reduction in the height to which the spatter particle jumps from the powder layer was also noticed in the images obtained from processing the ASLed powder.

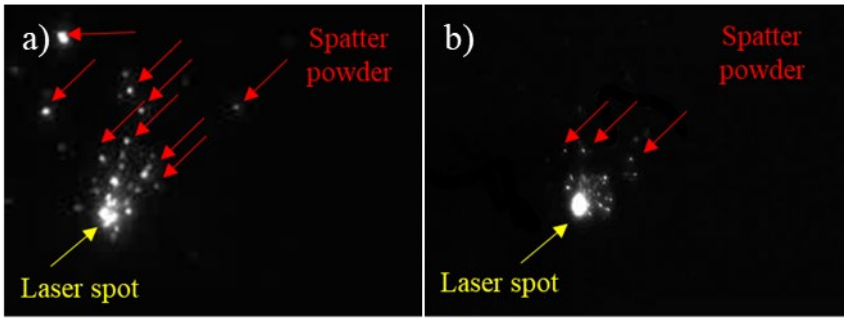

Figure 4. Comparison of laser spatters: (a) First run with as-received powder, and (b) second run with ASLed powder.

As demonstrated in figure 5, the distribution of the spatter particles has been obtained for the LPBF processing of as-received and ASLed powders. Each image obtained from either of the runs are picked and the spatter particles are manually counted. Using image J, area of each particles counted have been calculated. Particles of area less than 5 μm^2 was not considered because of the limitations due to resolution of the camera. For each particle area ranges, the number of spatter particles were lesser in ASLed powder when compared to as-received powder as it can be observed from figure 5. The particles within the area range of 5 and 505 μm^2 contributed to most of the spatter particles ejected. For spatter particles within the area range of 5 and 255 μm^2, the number of particles that were ejected was 318 for ASLed powder compared to 450 for the as-received powder and for particles within the area range of 255 and 505 μm^2, ASLed powder ejected 82 particles whereas as-received powder ejected 124 particles. These reductions made it clear for overall reduction in the spatter particles escaping out of the melt pool when ASL is used in the as-received powder. Though spatter particles of area greater than 2005 μm^2 was found, the amount of them were not significant. The biggest particle found was 7505 μm^2 in area.

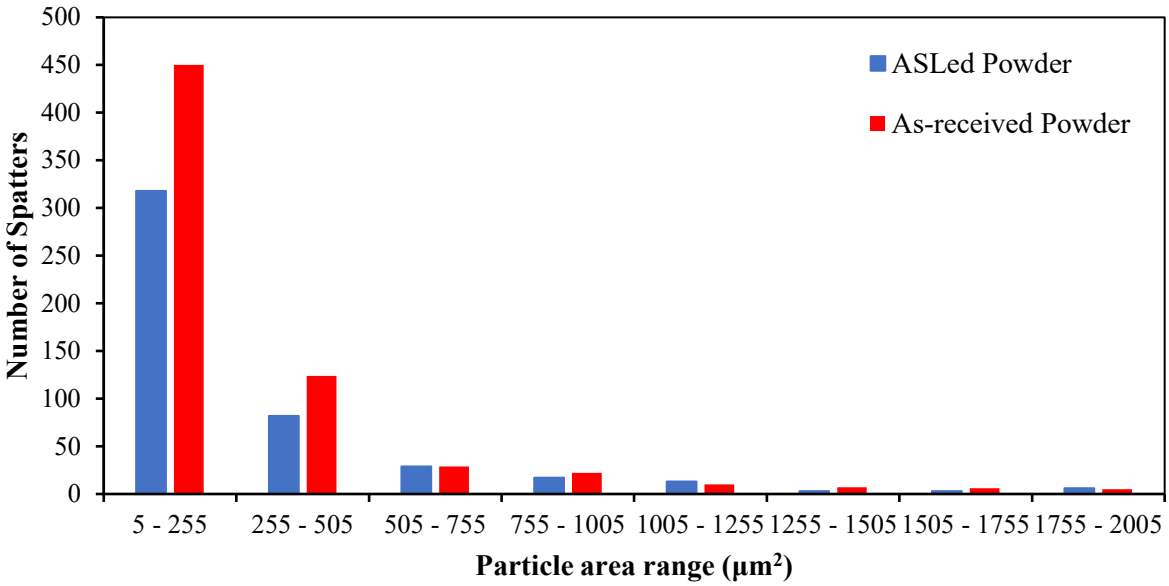

Figure 5. Particle area distribution of the as-received and ASLed Powders.

3.2 Microstructure Analysis

In order to study the changes in the Ti-6Al-4V as-received powder when ASL is sprayed, SEM and XRD analysis have been carried out on both the as-received and ASLed powders before processing the powder using laser. As shown in figure 6, comparing the SEM micrographs for both as-received and ASLed powder, few visual changes in the surface of the ASLed powder particles can be seen as indicated in the images.

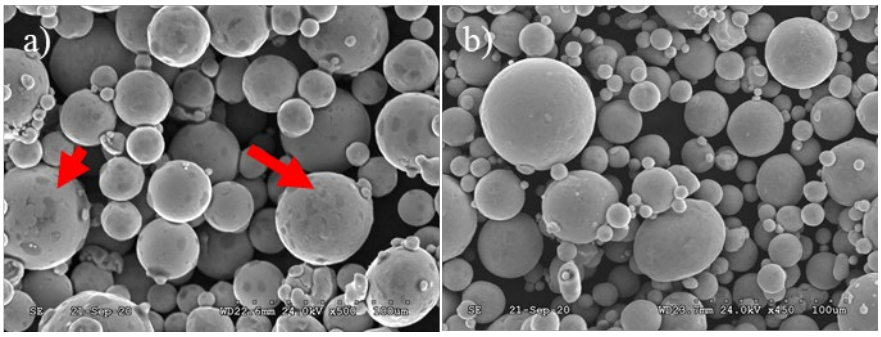

Figure 6. a) SEM image of ASLed powder and b) as-received powder.

3.3 Compositional analysis

XRD results shown in figure 7 compares the phases for the as-received powder with that of the ASLed powder. The graphs confirm that there was no significant deviation in the phases of the ASLed and as-received powder which could be used to confirm the fact that no significant changes in the composition of the ASL powder could be observed. It should be noted that the penetration depth of X-rays depends on the density, packing factor of powder, the mass absorption coefficient, the incident angle, and the wavelength of radiation. For this study, the average penetration depth was calculated to be 4 microns.

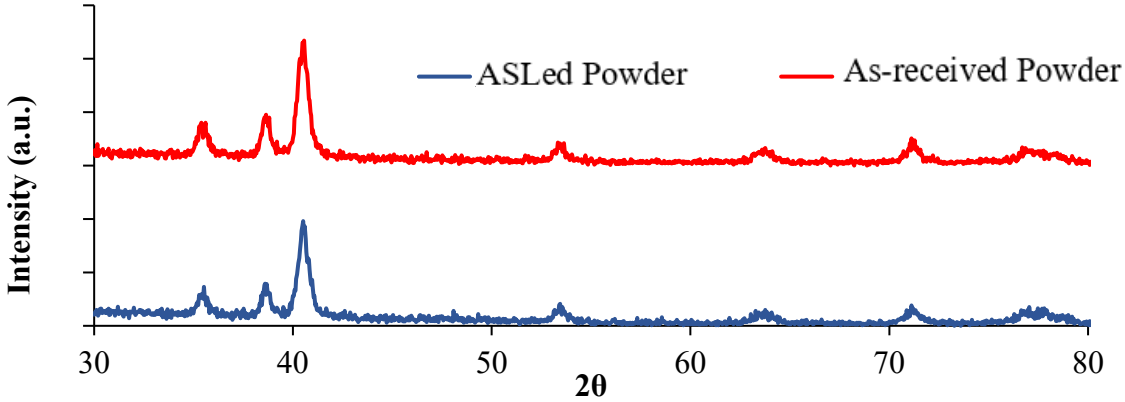

Figure 7. XRD results of the as-received and ASLed powders.

4. Conclusion

Single track laser LPBF runs have been successfully carried out over as-received Ti-6Al-4V and ASLed powders. High speed camera was employed to capture images at a specific frame rate and then were post-processed to clearly identify the spatter particles. It was concluded that the use of Anti-Spatter Liquid over the as received powder reduced the amount and area of the spatter particles ejected out of the molten metal. The microstructure characterization and composition analysis of the ASLed powder did not show any significant deviations compared to that of the as-received powder. The effect of controlling the quantity of ASL sprayed over as-received powder on the spatter behavior and sections of the powder bed typically prone toward spatter deposition will be studied in the future works.

5. Acknowledgment

This work was supported by a University of Texas System STARs award.

6. References

[1] C. Cui, B. Hu, L. Zhao, and S. Liu, "Titanium alloy production technology, market prospects and industry development," *Mater. Des.*, vol. 32, no. 3, pp. 1684–1691, Mar. 2011, doi: 10.1016/j.matdes.2010.09.011.

[2] S. Liu and Y. C. Shin, "Additive manufacturing of Ti6Al4V alloy: A review," *Mater. Des.*, vol. 164, p. 107552, Feb. 2019, doi: 10.1016/j.matdes.2018.107552.

[3] T. P. S. Sarao, H. Singh, and H. Singh, "Enhancing Biocompatibility and Corrosion Resistance of Ti-6Al-4V Alloy by Surface Modification Route," *J. Therm. Spray Technol.*, vol. 27, no. 8, pp. 1388–1400, Dec. 2018, doi: 10.1007/s11666-018-0746-7.

[4] P. Kumar, O. Prakash, and U. Ramamurty, "Micro-and meso-structures and their influence on mechanical properties of selectively laser melted Ti-6Al-4V," *Acta Mater.*, vol. 154, pp. 246–260, Aug. 2018, doi: 10.1016/j.actamat.2018.05.044.

[5] J. Suryawanshi, K. G. Prashanth, S. Scudino, J. Eckert, O. Prakash, and U. Ramamurty, "Simultaneous enhancements of strength and toughness in an Al-12Si alloy synthesized using selective laser melting," *Acta Mater.*, vol. 115, pp. 285–294, Aug. 2016, doi: 10.1016/j.actamat.2016.06.009.

[6] W. Xu, E. W. Lui, A. Pateras, M. Qian, and M. Brandt, "In situ tailoring microstructure in additively manufactured Ti-6Al-4V for superior mechanical performance," *Acta Mater.*, vol. 125, pp. 390–400, Feb. 2017, doi: 10.1016/j.actamat.2016.12.027.

[7] J.-R. Zhuang, Y.-T. Lee, W.-H. Hsieh, and A.-S. Yang, "Determination of melt pool dimensions using DOE-FEM and RSM with process window during SLM of Ti6Al4V powder," *Opt. Laser Technol.*, vol. 103, pp. 59–76, Jul. 2018, doi: 10.1016/j.optlastec.2018.01.013.

[8] D. Wang *et al.*, "Mechanisms and characteristics of spatter generation in SLM processing and its effect on the properties," *Mater. Des.*, vol. 117, pp. 121–130, Mar. 2017, doi: 10.1016/j.matdes.2016.12.060.

[9] T. Zhang *et al.*, "Evolution of molten pool during selective laser melting of Ti–6Al–4V," *J. Phys. Appl. Phys.*, vol. 52, no. 5, p. 055302, Nov. 2018, doi: 10.1088/1361-6463/aaee04.

[10] M. Taheri Andani, R. Dehghani, M. R. Karamooz-Ravari, R. Mirzaeifar, and J. Ni, "Spatter formation in selective laser melting process using multi-laser technology," *Mater. Des.*, vol. 131, pp. 460–469, Oct. 2017, doi: 10.1016/j.matdes.2017.06.040.

[11] V. Gunenthiram *et al.*, "Experimental analysis of spatter generation and melt-pool behavior during the powder bed laser beam melting process," *J. Mater. Process. Technol.*, vol. 251, pp. 376–386, Jan. 2018, doi: 10.1016/j.jmatprotec.2017.08.012.

[12] M. H. Nasab, D. Gastaldi, N. F. Lecis, and M. Vedani, "On morphological surface features of the parts printed by selective laser melting (SLM)," *Addit. Manuf.*, vol. 24, pp. 373–377, Dec. 2018, doi: 10.1016/j.addma.2018.10.011.

[13] C. A. Schneider, W. S. Rasband, and K. W. Eliceiri, "NIH Image to ImageJ: 25 years of image analysis," *Nat. Methods*, vol. 9, no. 7, pp. 671–675, Jul. 2012, doi: 10.1038/nmeth.2089.

[14] N. Otsu, “A Threshold Selection Method from Gray-Level Histograms,” *IEEE Trans. Syst. Man Cybern.*, vol. 9, no. 1, pp. 62–66, Jan. 1979, doi: 10.1109/TSMC.1979.4310076.